LA-UR- 98-4069

Approved for public release;
distribution is unlimited.

Title: FEEDBACK LINEARIZATION APPLICATION FOR LLRF CONTROL SYSTEM

CONF-990602--

Author(s): Sung-il Kwon, a. H. Regan, Y. M. Wang, A. S. Rohlev

Submitted to: American Control conf., San Diego, CA, June 2-4, 1999

Los Alamos
NATIONAL LABORATORY

Title: **Feedback linearization application for LLRF control system**

Authors: Sung-il Kwon, Amy Regan, Y. M. Wang, and T. Rohlev
RF Technology Group
Accelerator Operations and Technology Division
Los Alamos National Laboratory
E-mail: skwon@lanl.gov

Submitted to: 1999 American Control Conference, San Diego, CA.

Remark: The second sections of the paper entitled "Adaptive feedforward ..." , the paper entitled "Phase synchronization ...", and the paper entitled "Feedback linearization ..." are describing the klystron model and are almost same. Also, the third sections of the paper entitled "Adaptive feedforward ..." and the paper entitled "Feedback linearization ..." are describing the RF cavity model and almost same. The rest sections of each paper describe the different control techniques and they are derived from the klystron model and the RF cavity model described in the second section and the third section. When at least two papers are accepted for full papers, the second section and the third section will be modified.

Feedback linearization Application for LLRF Control System

Sung-il Kwon, Amy Regan, Y. M. Wang, and T. Rohlev
RF Technology Group
Accelerator Operations and Technology Division
Los Alamos National Laboratory
P.O.Box 1663
Los Alamos, NM 87544, USA
E-mail: skwon@lanl.gov

Abstract-The Low Energy Demonstration Accelerator(LEDA) being constructed at Los Alamos National Laboratory will serve as the prototype for the low energy section of Acceleration Production of Tritium(APT) accelerator. This paper addresses the problem of the LLRF control system for LEDA. We propose a control law which is based on exact feedback linearization coupled with gain scheduling which reduces the effect of the deterministic klystron cathode voltage ripple that is due to harmonics of the high voltage power supply and achieves tracking of desired set points. Also, we propose an estimator of the ripple and its time derivative and the estimates based feedback linearization controller.

1 Introduction

The low energy demonstration accelerator(LEDA) for the Production of Tritium(APT) is being built at Los Alamos National Laboratory. The primary function of the low level RF(LLRF) control system of LEDA is to control RF fields in the accelerating Cavity and maintain field stability within $\pm 1\%$ peak to peak amplitude error and 1° peak to peak phase error[8].

This paper addresses the problem of the LLRF control system used for LEDA. We propose a control law which is based on exact feedback linearization[3] coupled with gain scheduling[9],[10]. The purpose of exact feedback linearization coupled with gain scheduling is to reduce the effect of the deterministic cathode ripple that is due to harmonics of high voltage power supply[7] and is to achieve tracking of desired set points. Low frequency ripple does not deteriorate the current LLRF control system based on PID control method. As frequency of ripple increases, the effect of the ripple on the performance increases too. Simulation shows that 0.3% high voltage power supply ripple yields 1.05° at about $72kHz$ [5]and 1.0% high voltage power supply ripple yields 3.6° at about $120kHz$[12]. In order to suppress the high frequency ripple, the proposed controller makes use of not only the ripple but also the time derivative of the ripple. The usage of time derivative of the ripple improve the controller performance[10]. First, we assume that the deterministic cathode ripple is measurable and derive the controller. Second, we propose the ripple estimator which estimates the ripple signal itself and the time derivative of the ripple as well and derive the controller coupled with the ripple estimator. As is well known, in order to design the exact feedback linearization controller, the given system to be controlled must be well defined. Previous works[11], [13] modeled the klystron and RF Cavity used for LEDA. Our current work is based on the klystron model and RF Cavity model set up in Matlab/Simulink environment.

2 The Klystron Model

We consider a klystron model as shown in Figure 1.

It has two inputs, LLRF_I and LLRF_Q and two output HPRF_I and HPRF_Q. As intermediate outputs, Klystron has the normalized amplitude **N_AMPLITUDE** and the normalized phase **N_PHASE**.

The first stage of a klystron are linear systems called **FILTER AND AMPLIFIER**. Let u_1=LLRF_I and let u_2=LLRF_Q. Let x_1 and x_2 be outputs of the systems whose transfer function are given by

$$\frac{X_1(s)}{U_1(s)} = \frac{1}{3.54e^{-7}s+1} \tag{1}$$

$$\frac{X_2(s)}{U_2(s)} = \frac{1}{3.54e^{-7}s+1}. \tag{2}$$

In state space, transfer functions (1) and (2) are represented as

$$\dot{x}_1 = -a_1x_1 + a_1u_1 \tag{3}$$

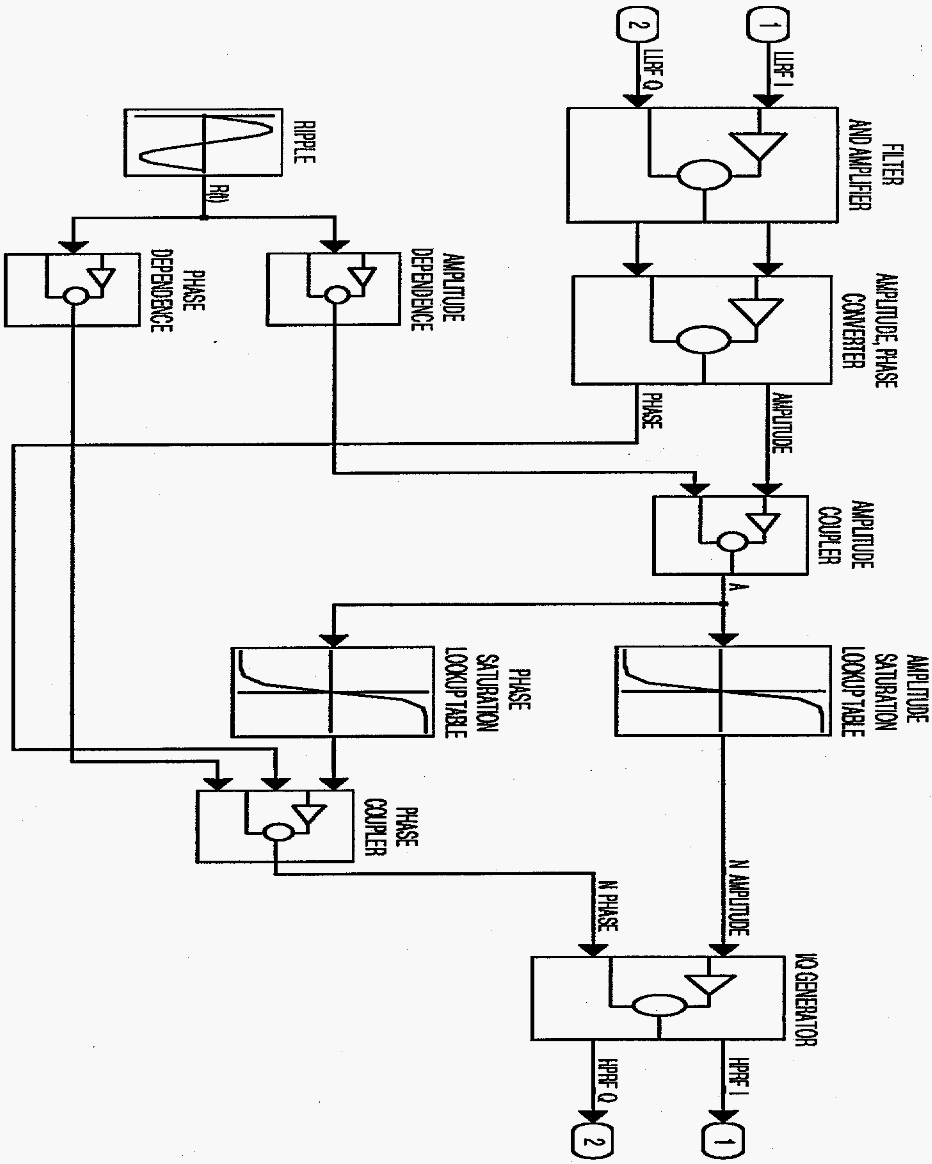

Figure 1: A Klystron Model

$$\dot{x}_2 = -a_1 x_2 + a_1 u_2 \tag{4}$$

where $a_1 = \frac{1e^{+007}}{3.54}$.

A klystron model has two loop-up tables, called **AMPLITUDE SATURATION** and **PHASE SATURATION**. The input of the two look-up tables is given by

$$A = \frac{K_g}{10\sqrt{KP_m}}(0.01R(t) + 1)^{1.25} \cdot \sqrt{x_1^2 + x_2^2} \tag{5}$$

where $R(t)$ is the ripple, K_g is the klystron gain, and KP_m is the maximum klystron power. $R(t)$, K_g, and KP_m are specified for a given klystron. For given A, the output of the look-up table **AMPLITUDE SATURATION** can be represented by

$$A_N = I_1(A) \tag{6}$$

and the output of the look-up table **PHASE SATURATION** can be represented by

$$\theta_N = I_2(A) \tag{7}$$

Table 1 and table 2 show data of look-up table **AMPLITUDE SATURATION** and data of look-up table **PHASE SATURATION**, respectively.

A	A_N	A	A_N	A	A_N	A	A_N
-0.1000	0.0000	0.0700	0.0000	0.1400	0.1900	0.5700	0.7500
0.7100	0.8700	0.8600	0.9800	0.9000	1.0000	0.9100	1.0000
0.3122	0.4143	0.3568	0.4724	0.4014	0.5305	0.4461	0.5886
0.4907	0.6467	0.5353	0.7048	0.5799	0.7585	0.5910	0.7680
1.0000	0.9900	0.4461	0.5886	0.6468	0.8158	0.6691	0.8349
0.0446	0.0000	0.0892	0.0521	0.6914	0.8540	0.7360	0.8891
0.1338	0.1732	0.1784	0.2400	0.7806	0.9218	0.8252	0.9545
0.2230	0.2981	0.2676	0.3562	0.8921	0.9961	0.9367	0.9970
0.3122	0.4143	0.3568	0.4724	0.9813	0.9921		

Table 1. AMPLITUDE SATURATION Data

A	θ_N	A	θ_N	A	θ_N	A	θ_N
-0.1000	0.0000	0.0700	0.0000	0.6400	-0.0150	0.7100	-0.0350
0.8600	-0.1370	0.9000	-0.2440	1.0000	-0.4770	0.0446	0.0000
0.4987	-0.0113	0.5445	-0.0125	0.5576	-0.0128	0.6691	-0.0233
0.0892	-5.0552e-4	0.1338	-0.0017	0.5712	-0.0132	0.7140	-0.0377
0.1784	-0.0029	0.2230	-0.0040	0.8921	-0.2229	0.4549	-0.0101
0.2676	-0.0052	0.3122	-0.0064	0.4483	-0.0100	0.4014	-0.0087
0.3568	-0.0075	0.7885	-0.0884	0.9593	-0.3821		

Table 2. PHASE SATURATION Data

The normalized amplitude N_Amplitude, defined by y_1^k and the normalized phase N_Phase, defined by y_2^k of the klystron are expressed by

$$y_1^k = A_N = I_1(A) \tag{8}$$

$$\begin{aligned} y_2^k &= \theta_N + tan^{-1}(\frac{x_2}{x_1}) + 3 \cdot \frac{\pi}{180} \cdot R(t) \\ &= I_2(A) + tan^{-1}(\frac{x_2}{x_1}) + 3 \cdot \frac{\pi}{180} \cdot R(t). \end{aligned} \tag{9}$$

In addition, for given y_1 and y_2, HPRF_I and HPRF_Q are given by

$$HPRF\_I = 10\sqrt{KP_m} \cdot y_1^k \cdot cos(y_2^k) \tag{10}$$

$$HPRF\_Q = 10\sqrt{KP_m} \cdot y_1^k \cdot sin(y_2^k). \tag{11}$$

Since the look-up tables have the limited number of data, we need to approximate the look-up tables by linear or nonlinear curve fitting equations. Considering the characteristic curve of a klystron, we choose nonlinear equations. We choose curve fitting equations of **AMPLITUDE SATURATION** and **PHASE SATURATION** having the forms

$$A_N = \sum_{i=1}^{N} c_i e^{-f_i A} \tag{12}$$

$$\theta_N = \sum_{i=1}^{N} d_i e^{-f_i A} \tag{13}$$

where f_i, $i = 1, 2, \cdots, N$ and parameters c_i, $i = 1, 2, \cdots, N$, d_i, $i = 1, 2, \cdots, N$ are to be determined.

Higher order of a curve fitting equation may yield more accurate curve fitting equation. For simplicity, we choose $N = 7$. Also, in order to reduce the number of coefficients to be determined, f_i, $i = 1, 2, \cdots, N$ are given in Table 3.

f_1	f_2	f_3	f_4	f_5	f_6	f_7
0.50	0.75	1.00	1.25	1.50	1.75	2.00

Table 3. Exponents of curve fitting equations

By using data given in Table 1 and Table 2, we obtain coefficients c_i, $i = 1, 2, \cdots, N$ and d_i, $i = 1, 2, \cdots, N$, of the curve fitting equations (12) and (13). Coefficients c_i and d_i obtained are given in Table 4. Figure 2 shows plots of data points as given in Table 4, Table 5 and plots of curve fitting equations (12) and (13) whose coefficients, f_i, $i = 1, 2, \cdots, N$, c_i, $i = 1, 2, \cdots, N$, d_i, $i = 1, 2, \cdots, N$, are given in Table 3 and Table 4 with appropriate domain of A.

c_1	0.05680429876058e+006	d_1	-0.14120739315590e+005
c_2	-0.39264357353961e+006	d_2	0.83084262097993e+005
c_3	1.12805594234952e+006	d_3	-2.01778226478032e+005
c_4	-1.72418545240933e+006	d_4	2.58441412755651e+005
c_5	1.47878241712872e+006	d_5	-1.83680595711727e+005
c_6	-0.67483667002473e+006	d_6	0.68453128529433e+005
c_7	0.12802296547207e+006	d_7	-0.10399245992504e+005

Table 4. Coefficients of curve fitting equations

Plugging (5) to (12) and (13), curve fitting equations (12) and (13) are reduced to

$$A_N = \sum_{i=1}^{N} c_i e^{-f_i w(t)\sqrt{x_1^2+x_2^2}} \tag{14}$$

$$\theta_N = \sum_{i=1}^{N} d_i e^{-f_i w(t)\sqrt{x_1^2+x_2^2}} \tag{15}$$

where

$$w(t) = \frac{K_g}{10\sqrt{KP_m}}(0.01R(t)+1)^{1.25}. \tag{16}$$

The normalized amplitude y_1^k and the normalized phase y_2^k of the klystron are

$$y_1^k = A_N = \sum_{i=1}^{N} c_i e^{-f_i w(t)\sqrt{x_1^2+x_2^2}} \tag{17}$$

$$\begin{aligned} y_2^k &= \theta_N + tan^{-1}(\frac{x_2}{x_1}) + 3 \cdot \frac{\pi}{180} \cdot R(t) \\ &= \sum_{i=1}^{N} d_i e^{-f_i w(t)\sqrt{x_1^2+x_2^2}} + tan^{-1}(\frac{x_2}{x_1}) + 3 \cdot \frac{\pi}{180} \cdot R(t). \end{aligned} \tag{18}$$

In addition, for given y_1^k and y_2^k, HPRF_I and HPRF_Q are given by

$$HPRF\_I = 10\sqrt{KP_m} \cdot y_1^k \cdot cos(y_2^k) \tag{19}$$

$$HPRF\_Q = 10\sqrt{KP_m} \cdot y_1^k \cdot sin(y_2^k). \tag{20}$$

2.1 The Klystron in z-coordinate

Consider the normalized amplitude y_1^k and the normalized phase y_2^k as given in (17) and (18).

Let

$$z_1 = \sqrt{x_1^2 + x_2^2} \tag{21}$$

$$z_2 = tan^{-1}(\frac{x_2}{x_1}). \tag{22}$$

We consider a transformation from x-coordinate to z-coordinate. In z-coordinate, the state equations (3) and (4) are reduced to

$$\dot{z}_1 = -a_1 z_1 + a_1 cos(z_2)u_1 + a_1 sin(z_2)u_2 \tag{23}$$

$$\dot{z}_2 = -a_1\frac{sin(z_2)}{z_1}u_1 + a_1\frac{cos(z_2)}{z_1}u_2. \tag{24}$$

Also, the curve fitting equations (12) and (13) are reduced to

$$A_N = \sum_{i=1}^{N} c_i e^{-f_i w(t) z_1} \tag{25}$$

$$\theta_N = \sum_{i=1}^{N} d_i e^{-f_i w(t) z_1}. \tag{26}$$

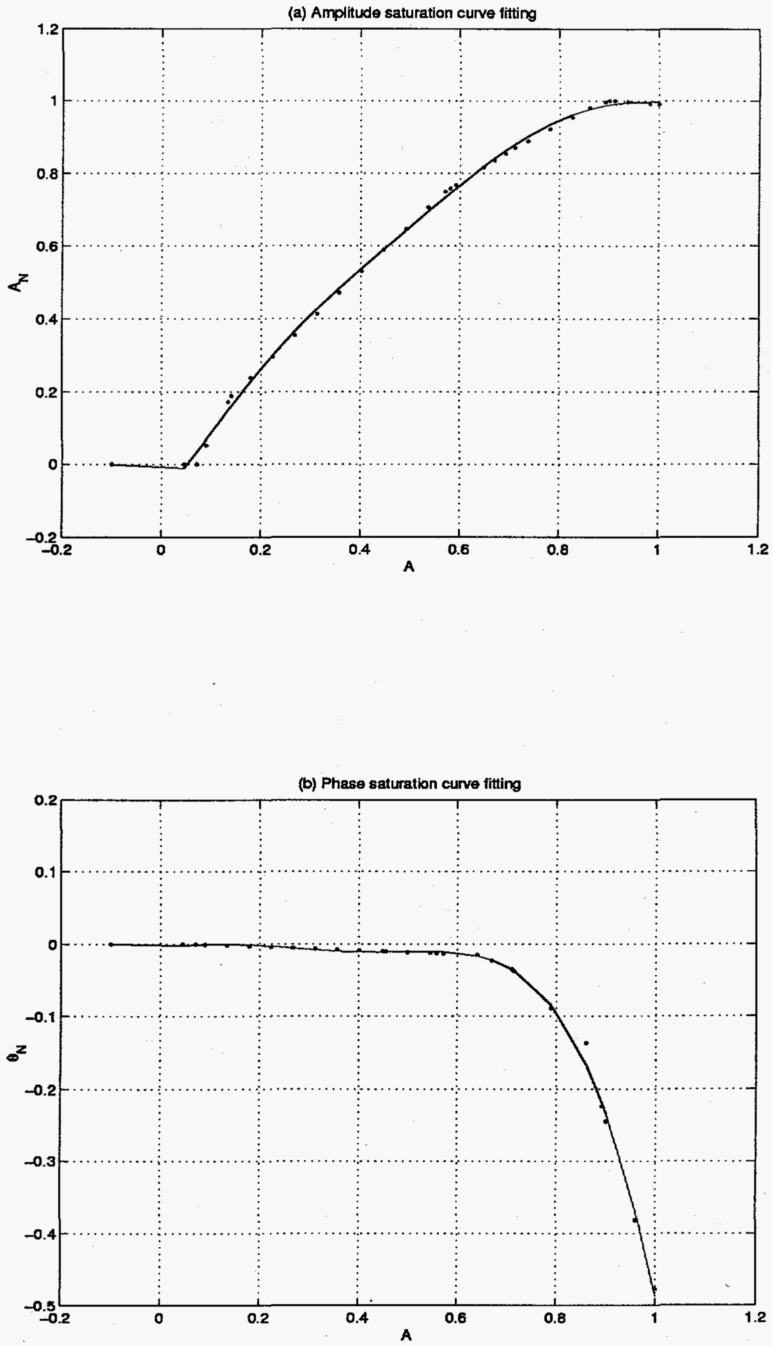

Figure 2: Curve fittings

The normalized amplitude y_1^k and the normalized phase y_2^k are represented by

$$y_1^k = \sum_{i=1}^{N} c_i e^{-f_i w(t) z_1} \tag{27}$$
$$y_2^k = \sum_{i=1}^{N} d_i e^{-f_i w(t) z_1} + z_2 + 3 \cdot \frac{\pi}{180} \cdot R(t). \tag{28}$$

Note that the exponents of the first term of (27) are the same as the exponents of the first term of (28). Also, note that the phase y_2^k is linear with respect to z_2.

3 The RF Cavity

Figure 3 shows the RF cavity.

RF Cavity has has four inputs, HPRF_I, HPRF_Q, BEAM_I, and BEAM_Q and two outputs, CAV_FLD_I, CAV_FLD_Q.

Let u_1^c=HPRF_I, u_2^c=HPRF_Q, u_3^c=BEAM_I, u_4^c=BEAM_Q and let y_1^c=CAV_FLD_I, y_2^c=CAV_FLD_ Then RF Cavity can be expressed in the state space form.

$$\dot{x} = Ax + Bu^c \tag{29}$$
$$y^c = Cx \tag{30}$$

where

$$A = \begin{bmatrix} a - \frac{1}{50}c_1 & b - \frac{1}{50}c_2 & 0 & 0 & 0 & 0 & \frac{1}{50}c_3 & \frac{1}{50}c_4 \\ 1 & 0 & 0 & 0 & 0 & 0 & 0 & 0 \\ -\frac{1}{50}c_1 & -\frac{1}{50}c_2 & a & b & 0 & 0 & \frac{1}{50}c_3 & \frac{1}{50}c_4 \\ 0 & 0 & 1 & 0 & 0 & 0 & 0 & 0 \\ 0 & 0 & -\frac{1}{50}c_3 & -\frac{1}{50}c_4 & a - \frac{1}{50}c_1 & b - \frac{1}{50}c_2 & 0 & 0 \\ 0 & 0 & 0 & 0 & 1 & 0 & 0 & 0 \\ 0 & 0 & -\frac{1}{50}c_3 & -\frac{1}{50}c_4 & -\frac{1}{50}c_1 & -\frac{1}{50}c_2 & a & b \\ 0 & 0 & 0 & 0 & 0 & 0 & 1 & 0 \end{bmatrix},$$

$$B = \begin{bmatrix} \frac{2}{50} & 0 & -2eta & 0 \\ 0 & 0 & 0 & 0 \\ \frac{2}{50} & 0 & -2eta & 0 \\ 0 & 0 & 0 & 0 \\ 0 & \frac{2}{50} & 0 & -2eta \\ 0 & 0 & 0 & 0 \\ 0 & \frac{2}{50} & 0 & -2eta \\ 0 & 0 & 0 & 0 \end{bmatrix},$$

$$C = \begin{bmatrix} c_1 & c_2 & 0 & 0 & 0 & 0 & -c_3 & -c_4 \\ 0 & 0 & c_3 & c_4 & c_1 & c_2 & 0 & 0 \end{bmatrix}$$

$$a = -\frac{2}{\tau}$$

$$b = -(\frac{1}{\tau^2} + KDW^2)$$

$$c_1 = \frac{KR}{\tau}$$

$$c_2 = \frac{KR}{\tau}(\frac{1}{\tau} - \frac{KDW}{2KQo})$$

$$c_3 = \frac{KR}{2\tau \cdot KQo}$$

$$c_4 = \frac{KR}{2\tau KQo}(\frac{1}{\tau} + 2KDW \cdot KQo).$$

Parameters of RF Cavity are given in [11].

Also, FLD_I and FLD_Q of the Cavity Field Sample System are given by

$$FLD\_I = FA \cdot cos(GD) \cdot y_1^c - FA \cdot sin(GD) \cdot y_2^c \tag{31}$$

$$FLD\_Q = FA \cdot sin(GD) \cdot y_1^c + FA \cdot cos(GD) \cdot y_2^c \tag{32}$$

and FLD_AMP and FLD_PHS of the Cavity Field Sample System are given by

$$FLD\_AMP = \sqrt{FLD\_I^2 + FLD\_Q^2}$$

$$FLD\_PHS = tan^{-1}(\frac{FLD\_Q}{FLD\_I})$$

where

$$FA = 0.00037809$$

$$GD = \frac{\pi}{180} \cdot (-0.039455).$$

The RF Cavity as given in (29), (30) is Hurwitz stable and is inverse stable as well.

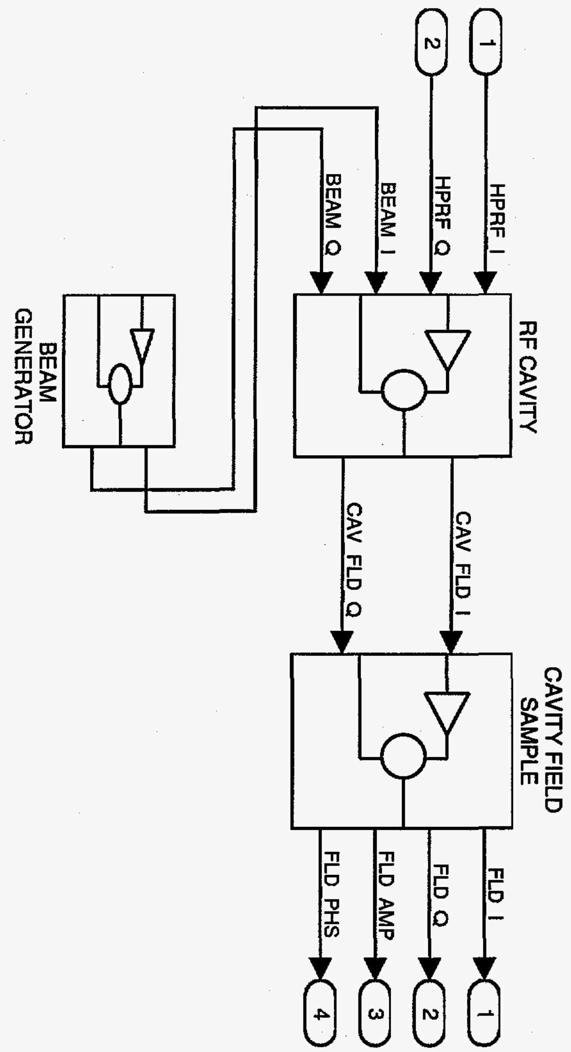

Figure 3: A RF Cavity Model and a Cavity Field Sample System

4 The Feedback Linearization Controller

Consider the Klystron equation in z-coordinate.

$$\dot{z}_1 = -a_1 z_1 + a_1 cos(z_2) u_1 + a_1 sin(z_2) u_2 \tag{33}$$

$$\dot{z}_2 = -a_1 \frac{sin(z_2)}{z_1} u_1 + a_1 \frac{cos(z_2)}{z_1} u_2. \tag{34}$$

and

$$y_1^k = \sum_{i=1}^{N} c_i e^{-f_i w(t) z_1} \tag{35}$$

$$y_2^k = \sum_{i=1}^{N} d_i e^{-f_i w(t) z_1} + z_2 + 3 \cdot \frac{\pi}{180} \cdot R(t) \tag{36}$$

where

$$w(t) = M(0.01R(t) + 1)^{1.25}$$

$$M = \frac{K_g}{10\sqrt{KP_m}}.$$

Define

$$\overline{z}_1 = (0.01R(t) + 1)^{1.25} z_1 \tag{37}$$

$$\overline{z}_2 = z_2 + 3 \cdot \frac{\pi}{180} \cdot R(t). \tag{38}$$

The Klystron is expressed in $\overline{z}$-coordinate by

$$\dot{\overline{z}}_1 = -\overline{a}_1 \overline{z}_1 + b_{z11}(\overline{z}, R(t), \dot{R}(t)) u_1 + b_{z12}(\overline{z}, R(t), \dot{R}(t)) u_2 + E_{z1}(R(t), \dot{R}(t)) \tag{39}$$

$$\dot{\overline{z}}_2 = b_{z21}(\overline{z}, R(t), \dot{R}(t)) u_1 + b_{z22}(\overline{z}, R(t), \dot{R}(t)) u_2 + E_{z2}(R(t), \dot{R}(t)) \tag{40}$$

$$y_1^k = \sum_{i=1}^{N} c_i e^{-f_i M \overline{z}_1} \tag{41}$$

$$y_2^k = \sum_{i=1}^{N} d_i e^{-f_i M \overline{z}_1} + \overline{z}_2. \tag{42}$$

where

$$\overline{a}_1 = a_1 - 0.0125(0.01R(t) + 1)^{-1} \dot{R}(t) \tag{43}$$

$$b_{z11}(\overline{z}, R(t), \dot{R}(t)) = a_1 (0.01R(t) + 1)^{1.25} cos(\overline{z}_2 - 3 \cdot \frac{\pi}{180} \cdot R(t)),$$

$$
\begin{aligned}
&b_{z12}(\overline{z}, R(t), \dot{R}(t)) = a_1(0.01R(t)+1)^{1.25} sin(\overline{z}_2 - 3\cdot\frac{\pi}{180}\cdot R(t)),\\
&b_{z21}(\overline{z}, R(t), \dot{R}(t)) = -a_1\frac{sin(\overline{z}_2 - 3\cdot\frac{\pi}{180}\cdot R(t))}{\overline{z}_1},\\
&b_{z22}(\overline{z}, R(t), \dot{R}(t)) = a_1\frac{cos(\overline{z}_2 - 3\cdot\frac{\pi}{180}\cdot R(t))}{\overline{z}_1},\\
&E_{z1}(R(t), \dot{R}(t)) = 0,\\
&E_{z2}(R(t), \dot{R}(t)) = 3\cdot\frac{\pi}{180}\dot{R}(t).
\end{aligned}
$$

Note that $\overline{B}_z(\overline{z}, R(t), \dot{R}(t))$ is invertible for any nonzero $\overline{z}_1$. In $\overline{z}$-coordinate, state equations are dependent upon the ripple $R(t)$ but the output equations are independent upon the ripple $R(t)$.

Define

$$
\overline{A}_z(R(t), \dot{R}(t)) = \begin{bmatrix} -\overline{a}_1 & 0 \\ 0 & 0 \end{bmatrix}, \tag{44}
$$

$$
\overline{z} = \begin{bmatrix} \overline{z}_1 \\ \overline{z}_2 \end{bmatrix}, \qquad u_z = \begin{bmatrix} u_1 \\ u_2 \end{bmatrix}, \tag{45}
$$

$$
E_z(R(t), \dot{R}(t)) = \begin{bmatrix} 0 \\ 3\cdot\frac{\pi}{180}\dot{R}(t) \end{bmatrix}, \tag{46}
$$

and

$$
\overline{B}_z(\overline{z}, R(t), \dot{R}(t)) = \begin{bmatrix} b_{z11}(\overline{z}, R(t), \dot{R}(t)) & b_{z12}(\overline{z}, R(t), \dot{R}(t)) \\ b_{z21}(\overline{z}, R(t), \dot{R}(t)) & b_{z22}(\overline{z}, R(t), \dot{R}(t)) \end{bmatrix}. \tag{47}
$$

Then, (39) and (40) are represented by

$$
\dot{\overline{z}} = \overline{A}_z(R(t), \dot{R}(t))\overline{z} + \overline{B}_z(\overline{z}, R(t), \dot{R}(t))u_z + E_z(R(t), \dot{R}(t)). \tag{48}
$$

Assume that $\overline{z}_1 \neq 0$. Define

$$
u_z = \overline{B}_z^{-1}(\overline{z}, R(t), \dot{R}(t))(\overline{u} - E_z). \tag{49}
$$

Then, (48) is reduced to

$$
\dot{\overline{z}} = \overline{A}_z(R(t), \dot{R}(t))\overline{z} + I_{2\times 2}\overline{u}. \tag{50}
$$

Let

$$\begin{aligned} \overline{u} &= K\overline{z} + R_z \\ &= \begin{bmatrix} k_1 + 0.0125(0.01R(t)+1)^{-1}\dot{R}(t) & 0 \\ 0 & k_2 \end{bmatrix} \overline{z} + \begin{bmatrix} r_1 \\ r_2 \end{bmatrix} \end{aligned} \tag{51}$$

where R_z is the control input that drives the steady state value $\overline{z}_s$ of $\overline{z}$ to the desired value of $\overline{z}$[2]. Then, (50) is reduced to

$$\dot{\overline{z}} = \overline{A}_{zc}\overline{z} + I_{2\times 2}R_z \tag{52}$$

where

$$\overline{A}_{zc} = \begin{bmatrix} -a_1 + k_1 & 0 \\ 0 & k_2 \end{bmatrix}. \tag{53}$$

$\overline{A}_{zc}$ is a constant matrix and is independent of $R(t)$ and $\dot{R}(t)$. By proper choice of k_1 and k_2, we can locate the eigenvalues of the matrix $\overline{A}_{zc}$ that what we want.

R_z is the solution of the following equation[2].

$$0 = \overline{A}_{zc}\overline{z}_s + I_{2\times 2}R_z. \tag{54}$$

The solution of (54) can be explained by the steady state value of the transfer function from R_z to $\overline{z}$. The transfer function from R_z to $\overline{z}$ is

$$\frac{\overline{z}(s)}{R_z(s)} = (sI - \overline{A}_{zc})^{-1}I_{2\times 2}.$$

For constant R_z, steady state value $\overline{z}_s$ of $\overline{z}$ is given by the equation

$$\overline{z}_s = (0I - \overline{A}_{zc})^{-1}I_{2\times 2}R_z$$

Equivalently,

$$0 = \overline{A}_{zc}\overline{z}_s + R_z.$$

The solution R_z of (54) is represented by the steady state value $\overline{z}_s$ of $\overline{z}$ and it is obtained as follow.

First, we consider the equations for FLD_I and FLD_Q as given in (31) and (32).

$$\begin{bmatrix} FLD\_I \\ FLD\_Q \end{bmatrix} = \begin{bmatrix} FA\cdot cos(GD) & -FA\cdot sin(GD) \\ FA\cdot sin(GD) & FA\cdot cos(GD) \end{bmatrix} \begin{bmatrix} y_1^c \\ y_2^c \end{bmatrix}. \tag{55}$$

Let FLD_I$_d$ and FLD_Q$_d$ be the desired values of FLD_I and FLD_Q. Then, the desired values y_{1d}^c, y_{2d}^c of y_1^c, y_2^c are given by the algebraic equation

$$\begin{bmatrix} y_{1d}^c \\ y_{2d}^c \end{bmatrix} = \begin{bmatrix} FA \cdot cos(GD) & -FA \cdot sin(GD) \\ FA \cdot sin(GD) & FA \cdot cos(GD) \end{bmatrix}^{-1} \begin{bmatrix} FLD\_I_d \\ FLD\_Q_d \end{bmatrix}. \tag{56}$$

Second, we consider the Cavity equation.

$$\dot{x} = Ax + Bu^c \tag{57}$$

$$y^c = Cx \tag{58}$$

Let $H_{CAV}(s)$ be the transfer function from u_1^c = HPRF_I and u_2^c = HPRF_Q to y_1^c = CAV_FLD_I and y_2^c = CAV_FLD_Q, assuming that u_3^c = BEAM_I and u_4^c = BEAM_Q are given and constant. Then, we obtain the relation represented by the transfer function $H_{CAV}(s)$

$$\begin{bmatrix} y_1^c(s) \\ y_2^c(s) \end{bmatrix} = H_{CAV}(s) \begin{bmatrix} u_1^c(s) \\ u_2^c(s) \end{bmatrix}. \tag{59}$$

Note that $H_{CAV}(s)$ has no zeros at the origin in the complex plane. Let $\overline{y}_1^c$, $\overline{y}_2^c$ be the steady state value of y_1^c, y_2^c, respectively and let $\overline{u}_1^c$, $\overline{u}_2^c$ be the steady state value of u_1^c, u_2^c, respectively. Then,

$$\begin{bmatrix} \overline{y}_1^c \\ \overline{y}_2^c \end{bmatrix} = H_{CAV}(0) \begin{bmatrix} \overline{u}_1^c \\ \overline{u}_2^c \end{bmatrix}. \tag{60}$$

$H_{CAV}(0)$ can be obtained by applying any steady state value test[1],[6]. One method is step input test[6]. Select u_1^{c1} as nonzero constant, u_2^{c1} as zero, and obtain y_1^{c1} and y_2^{c1}. Next, select u_1^{c2} as zero, u_2^{c2} as nonzero constant and obtain y_1^{c2} and y_2^{c2}. Then, $H_{CAV}(0)$ satisfies

$$\begin{bmatrix} y_1^{c1} & y_1^{c2} \\ y_2^{c1} & y_2^{c2} \end{bmatrix} = H_{CAV}(0) \begin{bmatrix} u_1^{c1} & u_1^{c2} \\ u_2^{c1} & u_2^{c2} \end{bmatrix}. \tag{61}$$

Since Cavity has no zeros at the origin in the complex plane,

$$\begin{bmatrix} \overline{u}_1^c \\ \overline{u}_2^c \end{bmatrix} = H_{CAV}^{-1}(0) \begin{bmatrix} \overline{y}_1^c \\ \overline{y}_2^c \end{bmatrix}. \tag{62}$$

Note that inputs u_1^c and u_2^c of Cavity are given by equations of the normalized amplitude y_1^k and the normalized phase y_2^k.

$$\begin{bmatrix} u_1^c \\ u_2^c \end{bmatrix} = \begin{bmatrix} 10\sqrt{KPm} \cdot y_1^k \cdot cos(y_2^k) \\ 10\sqrt{KPm} \cdot y_1^k \cdot sin(y_2^k) \end{bmatrix}. \tag{63}$$

Since Cavity has no zeros at the origin in the complex plane,

$$\begin{bmatrix} 10\sqrt{KPm} \cdot y_1^k \cdot cos(y_2^k) \\ 10\sqrt{KPm} \cdot y_1^k \cdot sin(y_2^k) \end{bmatrix} = H_{CAV}^{-1}(s) \begin{bmatrix} y_1^c \\ y_2^c \end{bmatrix}. \tag{64}$$

Let $\overline{y}_1^k$, $\overline{y}_2^k$ be the steady state values of y_1^k, y_2^k, respectively and let $\overline{y}_1^c$, $\overline{y}_2^c$ be the steady state values of y_1^c, y_1^c, respectively. Then, the steady state relation is given by

$$\begin{bmatrix} \overline{y}_1^k \cdot cos(\overline{y}_2^k) \\ \overline{y}_1^k \cdot sin(\overline{y}_2^k) \end{bmatrix} = \frac{1}{10\sqrt{KPm}} H_{CAV}^{-1}(0) \begin{bmatrix} \overline{y}_1^c \\ \overline{y}_2^c \end{bmatrix}. \tag{65}$$

Setting

$$\begin{bmatrix} \overline{y}_1^c \\ \overline{y}_2^c \end{bmatrix} = \begin{bmatrix} y_{1d}^c \\ y_{2d}^c \end{bmatrix},$$

and plugging (56) into (65), we obtain

$$\begin{bmatrix} \overline{y}_1^k \cdot cos(\overline{y}_2^k) \\ \overline{y}_1^k \cdot sin(\overline{y}_2^k) \end{bmatrix} = \frac{1}{10\sqrt{KPm}} H_{CAV}^{-1}(0) \begin{bmatrix} FA \cdot cos(GD) & -FA \cdot sin(GD) \\ FA \cdot sin(GD) & FA \cdot cos(GD) \end{bmatrix}^{-1} \begin{bmatrix} FLD\_I_d \\ FLD\_Q_d \end{bmatrix}. \tag{66}$$

Define the right-hand side of the above equation to be

$$\begin{bmatrix} \psi_1 \\ \psi_2 \end{bmatrix} = \frac{1}{10\sqrt{KPm}} H_{CAV}^{-1}(0) \begin{bmatrix} FA \cdot cos(GD) & -FA \cdot sin(GD) \\ FA \cdot sin(GD) & FA \cdot cos(GD) \end{bmatrix}^{-1} \begin{bmatrix} FLD\_I_d \\ FLD\_Q_d \end{bmatrix}. \tag{67}$$

Then,

$$\overline{y}_1^k = \sqrt{\psi_1^2 + \psi_2^2} \tag{68}$$

$$\overline{y}_2^k = tan^{-1}(\frac{\psi_2}{\psi_1}) \tag{69}$$

where $\overline{y}_1^k$ and $\overline{y}_2^k$ are the normalized amplitude and the normalized phase of Klystron which yield the desired value FLD_I$_d$ of FLD_I and the desired value FLD_Q$_d$ of FLD_Q.

The steady state values $\overline{z}_{1s}$, $\overline{z}_{2s}$, which are the desired values of $\overline{z}_1$, $\overline{z}_2$, respectively are obtained by solving the algebraic equations generated from (41),(42), (68) and (69).

$$\sum_{i=1}^{N} c_i e^{-f_i M \overline{z}_{1s}} = \overline{y}_1^k \tag{70}$$

$$\sum_{i=1}^{N} d_i e^{-f_i M \overline{z}_{1s}} + \overline{z}_{2s} = \overline{y}_2^k. \tag{71}$$

We have to solve $\overline{z}_{1s}$ and $\overline{z}_{2s}$. Instead of obtaining the analytic solution of the system (70) and (71), we obtain the numerical solution by resorting to an optimization method. Our approach is the minimization in the least square sense given as follow:

$$minimize \quad (\sum_{i=1}^{N} c_i e^{-f_i M \overline{z}_{1s}} - \overline{y}_1^k)^2 + (\sum_{i=1}^{N} d_i e^{-f_i M \overline{z}_{1s}} + \overline{z}_{2s} - \overline{y}_2^k)^2. \tag{72}$$

The controller design procedure is as follows:

Controller design procedure

1. Obtain $H_{CAV}(0)$ by applying a step input test.
2. Given desired FLD_I$_d$ and FLD_Q$_d$, obtain $\overline{y}_1^k$ and $\overline{y}_2^k$.
3. For the solutions $\overline{y}_1^k$ and $\overline{y}_2^k$, solve the optimization problem and obtain $\overline{z}_{1s}$ and $\overline{z}_{2s}$.
4. Obtain k_1 and k_2 so that the matrix $\overline{A}_{zc}$ is stable.
5. Find the solution R_z of $0 = \overline{A}_{zc}\overline{z} + R_z$.
6. Obtain the control input $\overline{u}$ as given in (51) and the control input u_z as given in (49).

5 Numerical Simulation

We consider the Klystron RF Cavity system when there is $20,000Hz$ sinusoidal ripple and $720Hz$, $120Hz$ ripples as well. The maximum power KP$_m$ and the klystron gain K$_g$ are given in Table 6.

K_g	8449.4
KP_m	3.600e+006

Table 6. Klystron gain and klystron maximum power

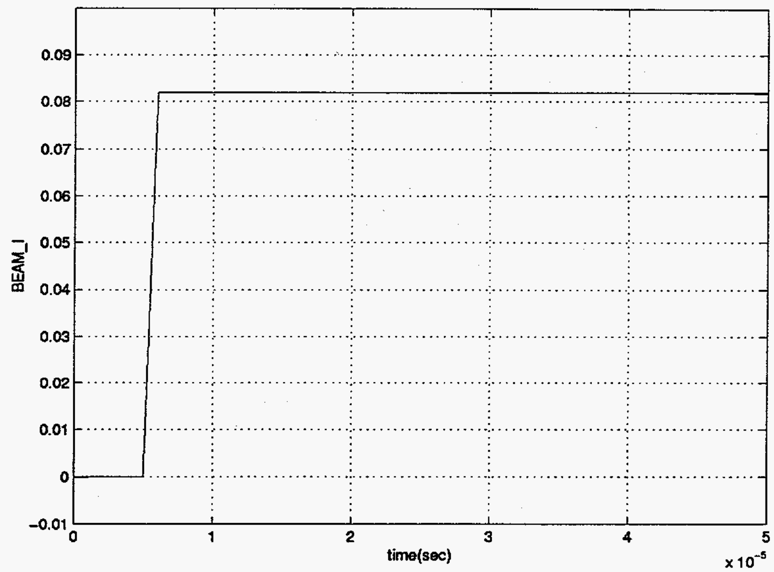

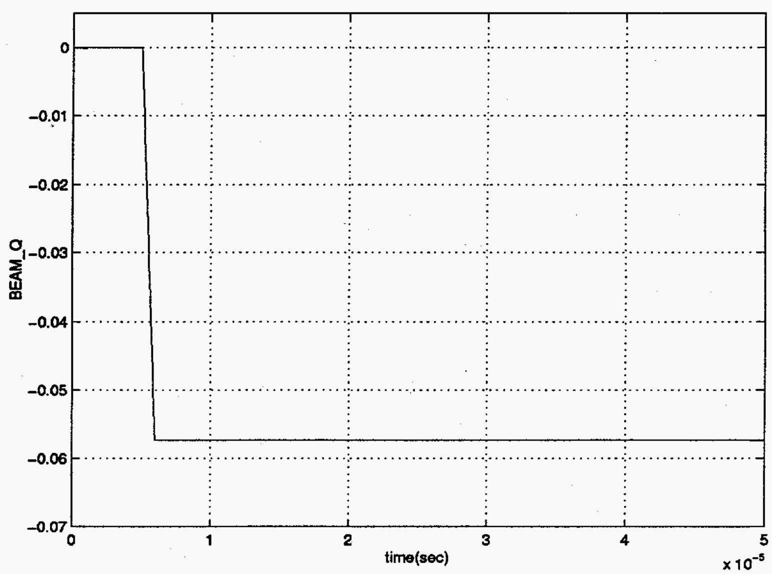

Figure 4: BEAM_I and BEAM_Q used for steady state gain simulation.

1. For steady state gain $H_{CAV}(0)$, we use the constant input method. BEAM_I and BEAM_Q used for the steady state gain simulation is in Figure 4.

   First, we set $\overline{u}_1^c = 13226.0$ and $\overline{u}_2^c = 0.0$. We simulated the RF Cavity and obtained the steady state values $\overline{y}_1^c$ and $\overline{y}_2^c$. Second, we set $\overline{u}_1^c = 0.0$ and $\overline{u}_2^c = 13226.0$. We simulated the RF Cavity and obtained the steady state values $\overline{y}_1^c$ and $\overline{y}_2^c$. Table 7 shows the results.

Simulation No.	$\overline{u}_1^c$	$\overline{u}_2^c$	$\overline{y}_1^c$	$\overline{y}_2^c$
1	13226.0	0.0	1.32243e+004	-1.75200e+000
2	0.0	13226.0	-1.91973e+002	1.74330e+004

Table 7. Steady state gain simulation

   From the simulation results as given in Table 7, we compute the steady state gain $H_{CAV}(0)$.

$$H_{CAV}(0) = \begin{bmatrix} 0.99987 & -0.01452 \\ -0.00013 & 1.31809 \end{bmatrix}.$$

2. Let the desired FLD_I$_d$ and FLD_Q$_d$ be FLD_I$_d$ = 5.0 and FLD_Q$_d$ = 0.0. From (67), (68), and (69), we obtain $\overline{y}_1^k$ and $\overline{y}_2^k$ as given in Table 8.

$\overline{y}_1^k$	6.97080e-001
$\overline{y}_2^k$	6.22858e-004

Table 8. Steady state normalized Amplitude $\overline{y}_1^k$ and the normalized phase $\overline{y}_2^k$

3. In order to solve the optimization problem (72), we made use of the unconstrained optimization algorithm in Matlab Toolbox. With initial values $\overline{z}_{1s} = 1.0$ and $\overline{z}_{2s} = 1.0$, after 54 iterations, we obtain the optimal solution $\overline{z}_{1s}$ and $\overline{z}_{2s}$ as given in Table 9.

$\overline{z}_{1s}$	1.20825
$\overline{z}_{2s}$	0.01088

Table 9. The solution $\overline{z}_{1s}$ and $\overline{z}_{2s}$ of the optimization problem (72)

4. Since $a_1 = 2.82486e{+}006$ is sufficiently large, we set $k_1 = -2.0a_1$. And we set $k_2 = -10a_1$. Hence, the eigenvalues of $\overline{A}_{zc}$ are $\lambda_1 = -3a_1$ and $\lambda_2 = -10a_1$ for any $R(t)$ and $\dot{R}(t)$.

5. The solution R_z of (54) is given by

$$R_z = \begin{bmatrix} 3.41312e + 006 \\ 3.07291e + 005 \end{bmatrix}.$$

Based on numerical values obtained, we implement the controller (50) to drive the Klystron-RF Cavity system.

Figure 5 through Figure 7 show the simulation results of the Klystron-RF Cavity system in Matlab/Simulink environment.

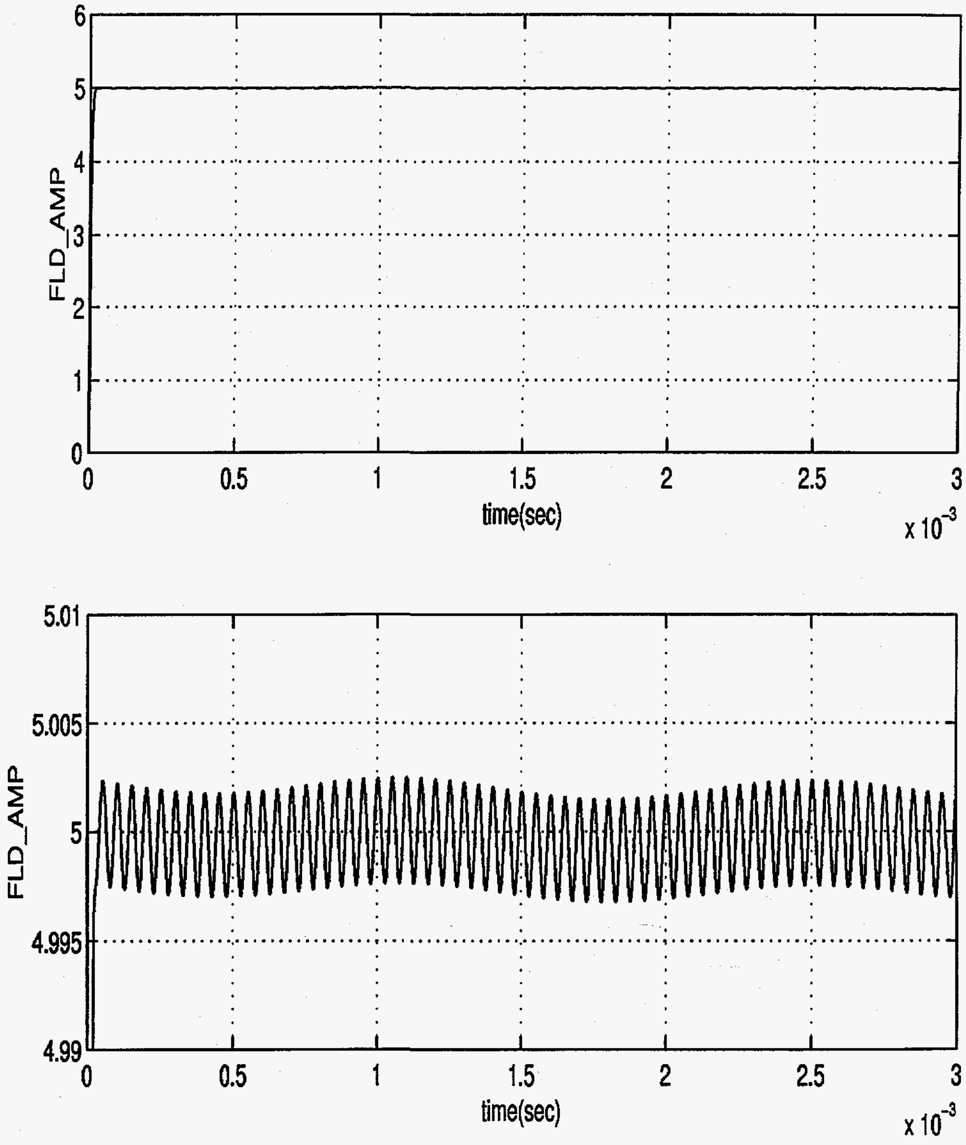

Figure 5: Field Amplitude, FLD_AMP

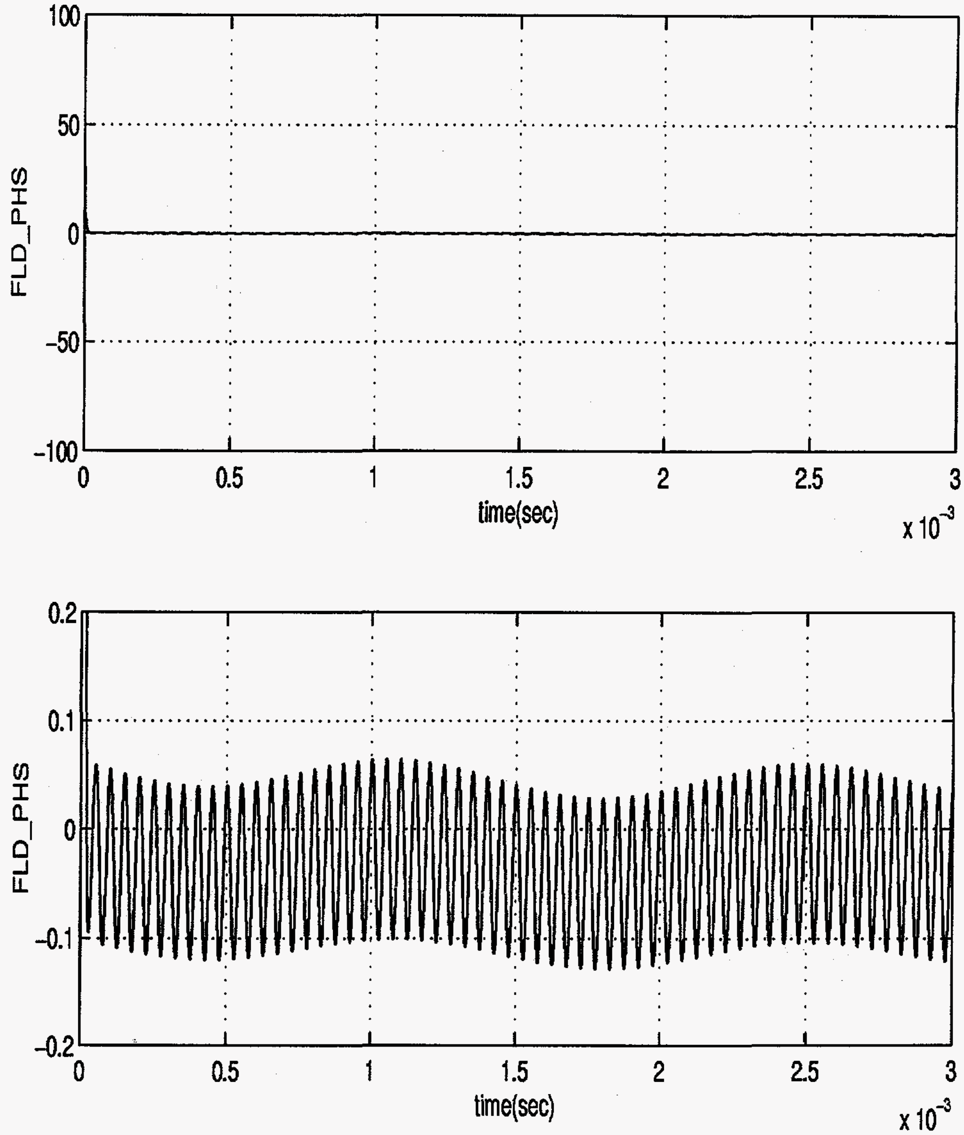

Figure 6: Field Phase, FLD_PHS

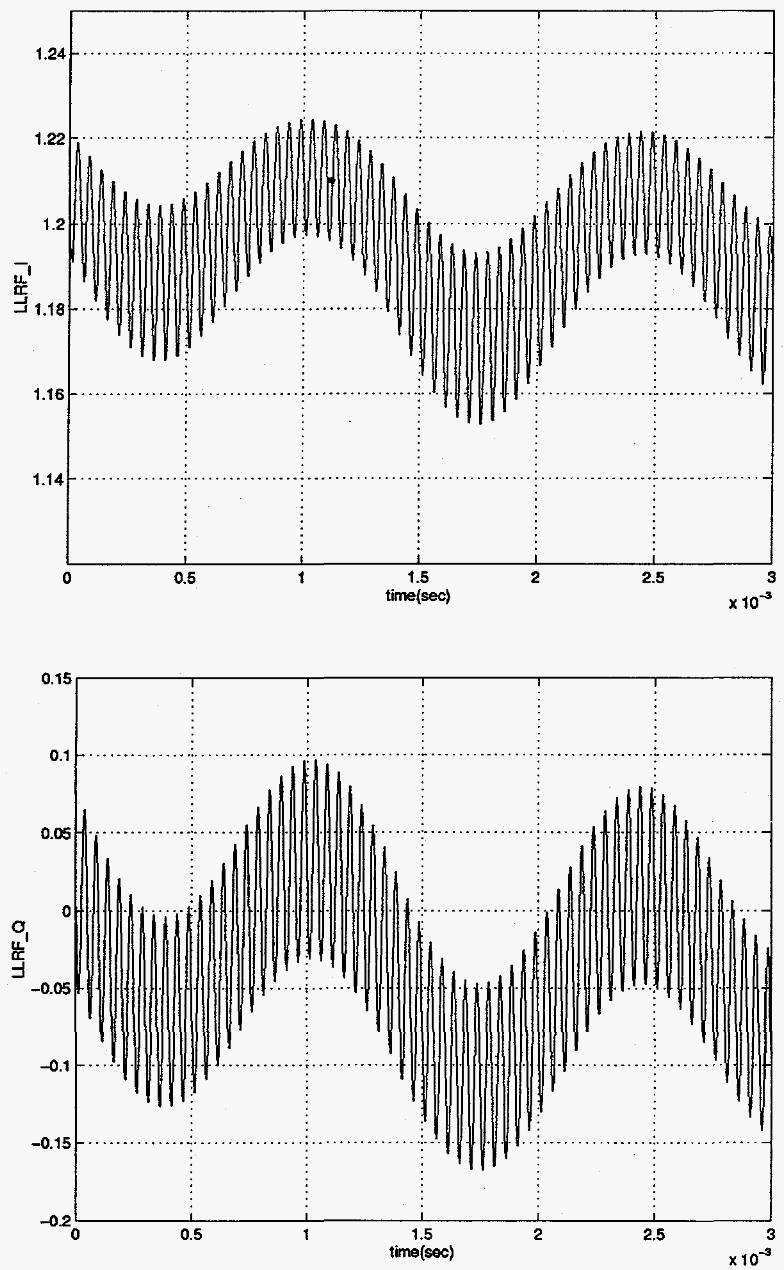

Figure 7: Control input LLRF_I and LLRF_Q

6 RIPPLE Estimation

The controller proposed in the previous section is based on the assumption that the information on ripple $R(t)$ and its time derivative $\frac{dR(t)}{dt}$ are fully known. When a designer has poor information on $R(t)$ and $\frac{dR(t)}{dt}$, the feedback linearization cannot give desired performance. Table 10 and Table 11 show amplitude and phase errors when there are phase difference and amplitude difference between the ripple used for controller and the real ripple entered a klystron. Table 10 is the results when there is a phase difference between the ripple of the feedback linearization controller and the ripple of the klystron. The controller ripple is $R(t) = sin(2\pi ft)$ and the ripple of the klystron is $R(t) = sin(2\pi ft + \phi)$, $f = 120KHz$. Here, ϕ is the phase of the ripple of klystron.

Ripple phase $\phi(rad)$	peak-to-peak field Phase error(Degrees)	peak-to-peak field Amplitude error(Volts)
0.0	0.00610	0.00006(0.00115 %)
$\frac{\pi}{8}$	1.12830	0.02368(0.47 %)
$\frac{2\pi}{8}$	2.21690	0.04000(0.80 %)
$\frac{4\pi}{8}$	4.10113	0.08600(1.72 %)

Table 10. Amplitude error and Phase error when there is difference in phase of ripple $R(t)$

Table 11 is the results when there is amplitude difference between the ripple of the feedback linearization controller and the ripple of the klystron. The controller ripple is $R(t) = A_R sin(2\pi ft)$, $A_R = 1.0$, $f = 120KHz$ and the ripple of the klystron is $R(t) = A_k sin(2\pi ft)$, $f = 120KHz$. Here, A_k is the amplitude of the ripple of klystron.

Klystron Ripple amplitude A_k	peak-to-peak field Phase error(Degrees)	peak-to-peak field Amplitude error(Volts)
0.6	1.16286	0.02432(0.49 %)
0.8	0.58323	0.01219(0.24 %)
1.2	0.57660	0.01209(0.24 %)
1.4	1.15631	0.02423(0.49 %)

Table 11. Amplitude error and Phase error when there is difference in amplitude of ripple $R(t)$

The purpose of the low level RF control(LLRF) system is to maintain the field stability within $\pm 1.0\%$ amplitude and $1.0°$ phase. In the case that there is phase difference, only $\frac{\pi}{8}$ phase difference yields $1.12°$ field phase error. In the case that there is amplitude difference, 40% gap of amplitude yields $1.156°$ field phase error.

For the remedy to the poor information on the ripple and its time derivative, we can make use of Lyapunov redesign after we design the exact feedback linearization controller based on the nominal values of the ripple and its time derivative[4]. This additional controller compensates the uncertainties or unmodelled dynamics. Another possible remedy is to design the estimator which yields the estimated ripple and its time derivative and based on the estimated information, we design the controller.

In this section, we address the ripple estimator which estimates the ripple $R(t)$ and its time derivative $\frac{dR(t)}{dt}$, and the feedback linearization controller based on the estimator.

We first consider equations as given in (21) and (22).

$$z_1 = \sqrt{x_1^2 + x_2^2} \tag{73}$$

$$z_2 = tan^{-1}(\frac{x_2}{x_1}) \tag{74}$$

where x_1 and x_2 satisfy

$$\dot{x}_1 = -a_1 x_1 + a_1 u_1 \tag{75}$$

$$\dot{x}_2 = -a_1 x_2 + a_1 u_2 \tag{76}$$

and u_1=LLRF_I, u_2=LLRF_Q. Given LLRF_I and LLRF_Q, we can obtain z_1 and z_2 by solving differential equations (75), (76) and algebraic equations (73), (74).

Second, we consider equations given by (19) and (20)

$$HPRF\_I = 10\sqrt{KP_m} \cdot y_1^k \cdot cos(y_2^k) \tag{77}$$

$$HPRF\_Q = 10\sqrt{KP_m} \cdot y_1^k \cdot sin(y_2^k). \tag{78}$$

From (77) and (78), for given HPRF_I and HPRF_Q, we obtain the normalized amplitude y_1^k and the normalized phase y_2^k of the klystron by solving algebraic equations.

$$y_1^k = \frac{1}{10\sqrt{KP_m}}\sqrt{HPRF\_I^2 + HPRF\_Q^2} \tag{79}$$

$$y_2^k = tan^{-1}(\frac{HPRF\_Q}{HPRF\_I}). \tag{80}$$

Third, we consider the klystron model as given in Figure 1. In Figure 1, the normalized amplitude of the klystron is the output of the look-up table **AMPLITUDE SATURA-**

TION and the input of the look-up table **AMPLITUDE SATURATION** is given by

$$A = \frac{K_g}{10\sqrt{KP_m}}(0.01R(t)+1)^{1.25} \cdot z_1 \tag{81}$$

in z-coordinate, or

$$A = \frac{K_g}{10\sqrt{KP_m}}\overline{z}_1 \tag{82}$$

in $\overline{z}$-coordinate. Also, there exists a region of (A, y_1^k) pairs where there is an inverse look-up table of the look-up table **AMPLITUDE SATURATION**. This region can be extracted from data given in Table 1 and Table 2. As in the case of **AMPLITUDE SATURATION**, we obtain the curve fitting equation for the inverse look-up table for **AMPLITUDE SATURATION**. Since in the controller design, we make use of the output equations (35) and (36) or (41) and (42) which are based on the curve fitting equation, we use the output equation as given in (41) in order to obtain the curve fitting equation for the inverse look-up table for **AMPLITUDE SATURATION** within the region of invertibility. Based on the generated data pairs from (41) where the selected data of y_1^k and $\overline{z}_1$ guarantee invertibility, we obtain the curve fitting equation as follows.

$$\overline{z}_1 = \sum_{i=1}^{N} c_i^z e^{-f_i^z y_1^k} \tag{83}$$

where $N = 7$, coefficients f_i^z, $i = 1, 2, \cdots, N$ and the coefficients c_i^z, $i = 1, 2, \cdots, N$ obtained are given in the Table 12.

f_1^z	0.50	c_1^z	246379.701273592
f_2^z	0.75	c_2^z	-1633291.85956396
f_3^z	1.00	c_3^z	4505197.57531207
f_4^z	1.25	c_4^z	-6618176.95439792
f_5^z	1.50	c_5^z	5460679.73050349
f_6^z	1.75	c_6^z	-2399431.11098975
f_7^z	2.00	c_7^z	438643.015066461

Table 12. Coefficients of Curve fitting equation for Inverse **AMPLITUDE SATURATION**

The estimate of the ripple $R(t)$ and the estimate of the time derivative $\frac{dR(t)}{dt}$ of the ripple $R(t)$ are obtained by considering the klystron system both in z-coordinate and $\overline{z}$-coordinate. The relationship between z-coordinate and $\overline{z}$-coordinate is given by

$$\overline{z}_1 = (0.01R(t) + 1)^{1.25} z_1 \tag{84}$$

$$\overline{z}_2 = z_2 + 3 \cdot \frac{\pi}{180} \cdot R(t). \tag{85}$$

Whenever x_1 and x_2 are obtained from (75) and (76), then we can obtain z_1 by using (73). Similarly, whenever y_1^k is obtained from (79), we can obtain $\overline{z}_1$ by using (83). For given z_1 and $\overline{z}_1$, we can obtain the estimate $\hat{R}(t)$ of the ripple $R(t)$ by solving algebraic equation (84).

$$\hat{R}(t) = 100((\frac{\overline{z}_1(t)}{z_1(t)})^{0.8} - 1.0). \tag{86}$$

Also, the estimate $\dot{\hat{R}}(t)$ of time derivative $\dot{R}(t)$ of the ripple $R(t)$ is obtained by differentiation of $\hat{R}(t)$.

The feedback linearization controller based on the estimate $\hat{R}(t)$ and $\dot{\hat{R}}(t)$ is given by

$$u_z = \hat{\overline{B}}_z^{-1}(\overline{z}, \hat{R}(t), \dot{\hat{R}}(t))(\overline{u} - E_z(\hat{R}(t), \dot{\hat{R}}(t))) \tag{87}$$

$$\overline{u} = \hat{K}(\hat{R}(t), \dot{\hat{R}}(t))\overline{z} + R_z, \tag{88}$$

where

$$\hat{\overline{B}}_z(\overline{z}, \hat{R}(t), \dot{\hat{R}}(t)) = \begin{bmatrix} b_{z11}(\overline{z}, \hat{R}(t), \dot{\hat{R}}(t)) & b_{z12}(\overline{z}, \hat{R}(t), \dot{\hat{R}}(t)) \\ b_{z21}(\overline{z}, \hat{R}(t), \dot{\hat{R}}(t)) & b_{z22}(\overline{z}, \hat{R}(t), \dot{\hat{R}}(t)) \end{bmatrix}, \tag{89}$$

$$E_z(\hat{R}(t), \dot{\hat{R}}(t)) = \begin{bmatrix} 0 \\ 3 \cdot \frac{\pi}{180}\dot{\hat{R}}(t) \end{bmatrix}, \tag{90}$$

$$\hat{K}(\hat{R}(t), \dot{\hat{R}}(t)) = \begin{bmatrix} k_1 + 0.0125(0.01\hat{R}(t) + 1)^{-1}\dot{\hat{R}}(t) & 0 \\ 0 & k_2 \end{bmatrix}, \tag{91}$$

$$R_z = \begin{bmatrix} r_1 \\ r_2 \end{bmatrix}. \tag{92}$$

Figure 8 shows the feedback linearization system in Matlab/Simulink environment. KLYSTRON is the klystron model, RIPPLE is the equivalent system which generates high voltage power supply ripple. RF_CAVITY is the RF Cavity with Beam. Inputs of the ripple estimator are HPRF_I, HPRF_Q, LLRF_I and LLRF_Q which are measurable. The ripple estimator estimates both the ripple and its time derivative. The time derivative information is used in the feedback linearization controller and the usage of the time derivative information improves the closed loop performance[10].

Figures 9-12 show the simulation when there is $20,000Hz$ sinusoidal ripple and $720Hz$, $120Hz$ ripples as well.

Figures 13-16 show the simulation when the ripple is

$$R(t) = 1.0sin(2\pi f_1 t) + 1.0sin(2\pi f_2 t + \frac{3\pi}{8})$$

where $f_1 = 120kHz$, $f_2 = 80kHz$.

References

[1] K. J. Astrom and T. Hagglund, *PID controllers:theory, design, and tuning*, Second Edition, Instrument Society of America, Research Triangle Park, NC, 1995.

[2] C.T. Chen, *Introduction to linear System Theory*, Second edition, Rinehart and Winston, New York, 1986.

[3] A. Isidori, *Nonlinear Control Systems*, Third Edition, Springer Verlag, New York, 1995.

[4] H.K. Khalil, *Nonlinear systems*, Macmillan, New York, 1992.

[5] S. Kwon, " 0.3% high voltage power supply ripple response test," *preprint.*

[6] Z. J. Palmor, Y. Halevi, and N. Krasney, "Automatic tuning of decentralized PID controllers for TITO processes," *Automatica*, vol. 31, pp. 1001-1010, 1995.

[7] D. Rees, J. Bradley III, K. Cummings, M. Lynch, A. Regan, T. Rohlev, W. Roybal, Y.M. Wang, "Design and test results of the low energy demonstration accelerator(LEDA) RF systems," *presented in XIX International LINAC Conference*, Chicago, USA, 1998.

[8] A. Regan and C. Ziomek, "APT LLRF control system model results," *presented in XIX International LINAC Conference*, Chicago, USA, 1998.

[9] W. J. Rugh, "Analytical Framework for Gain Scheduling," *IEEE Control Syst. Mag.*, vol. 11, no. 1, pp. 79-84, 1991.

[10] N. Sureshbabu and W. J. Rugh, "Output Regulation with Derivative Information," *IEEE Trans. Automat. Contr.*, vol. 40, pp. 1755-1766, 1995.

[11] C. Ziomek and A. Regan, "Simplification of Matrixx Model: Preliminary LLRF System Design," *Technical Note*, AOT-5-TN:001, RF Technology Group, AOT Division, Los Alamos National Laboratory, 1996.

[12] C. Ziomek and A. Regan, "Superconducting system model; HVPS ripple model," *Technical Note*, AOT-5-TN:003, RF Technology Group, AOT Division, Los Alamos National Laboratory, 1996.

[13] C. Ziomek and A. Regan, "Model Multiple Klystrons, Pulsed Beam (SC and NC)," *Technical Note*, AOT-5-TN:005, RF Technology Group, AOT Division, Los Alamos National Laboratory, 1996.

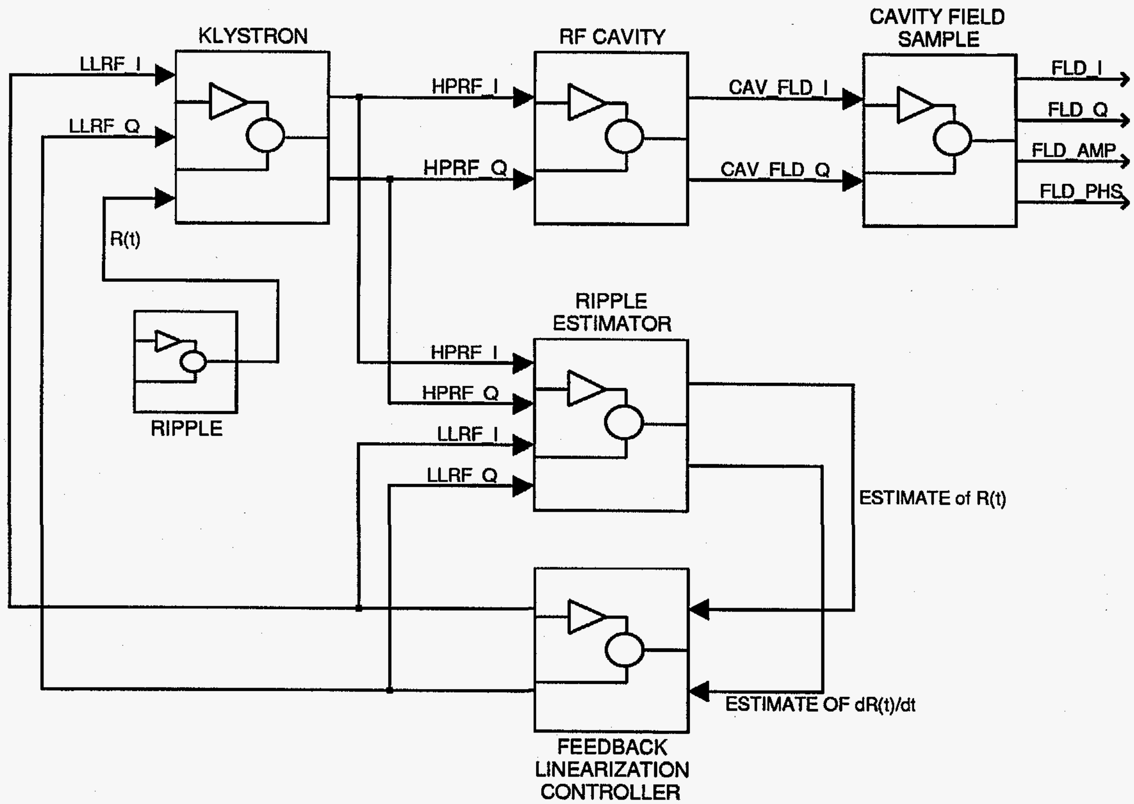

Figure 8: The feedback linearization system with ripple estimator

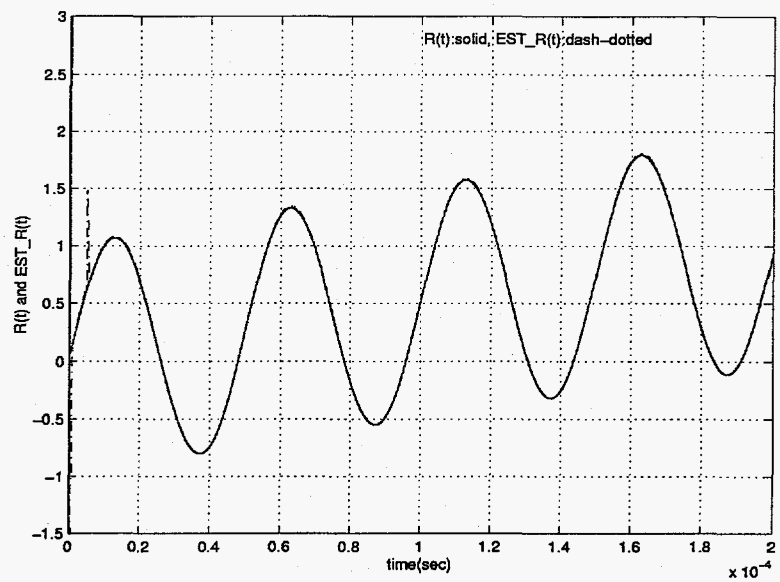

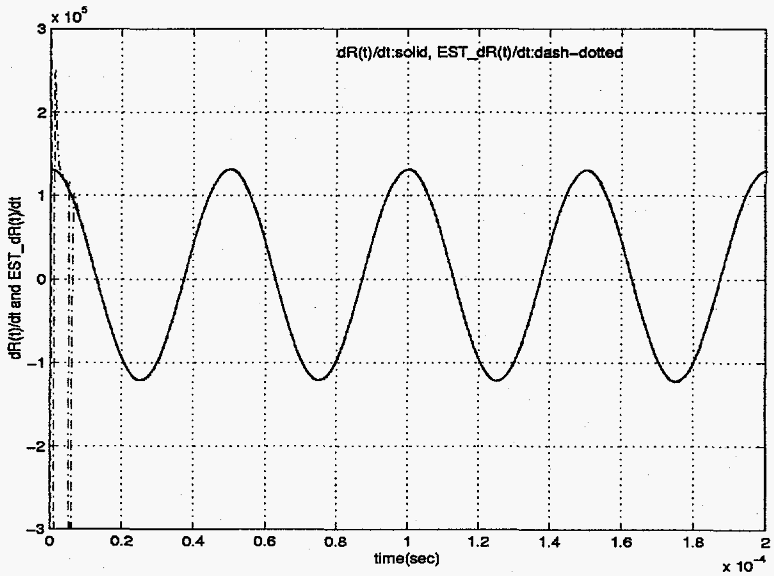

Figure 9: Ripple $R(t)$ and its time derivative $dR(t)/dt$ and their estimates $EST\_R(t)$ and $EST\_dR(t)/dt$

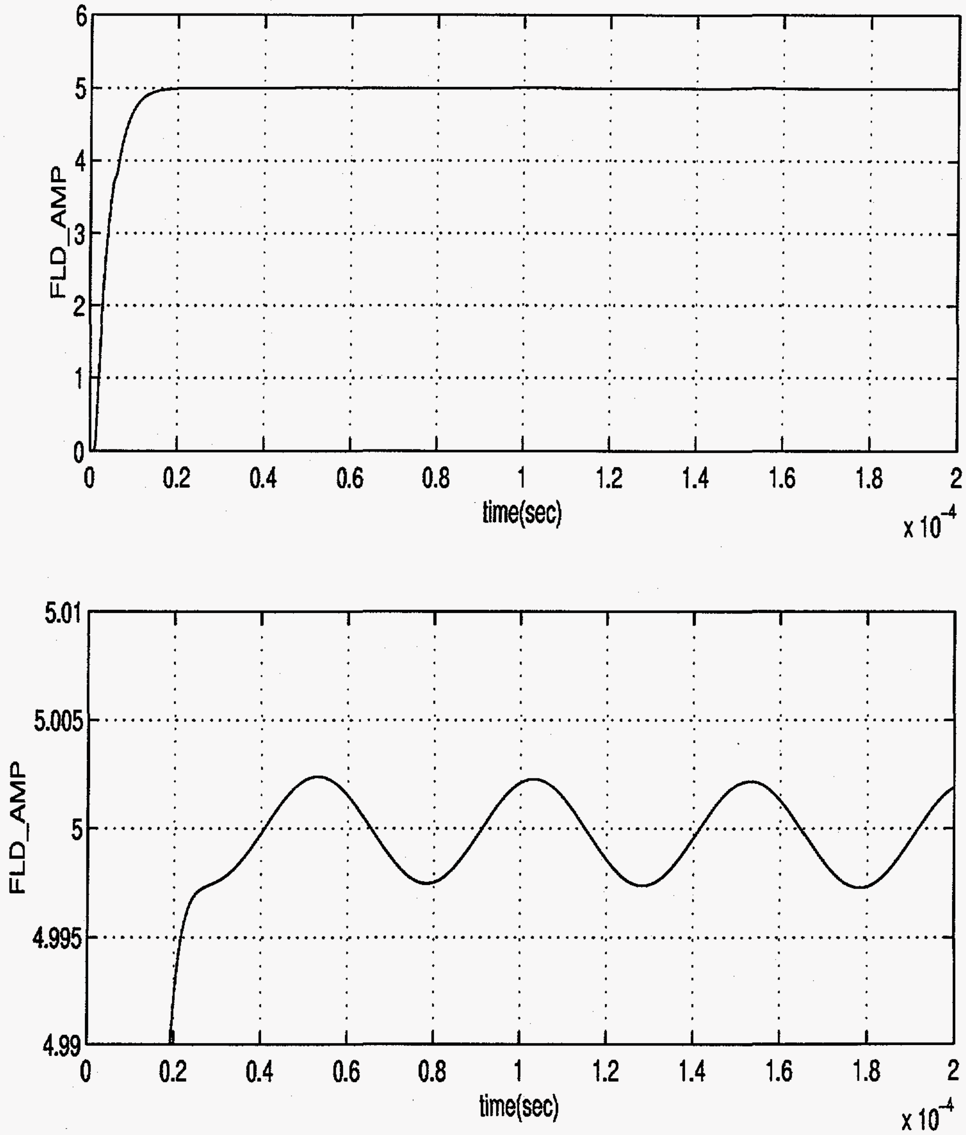

Figure 10: Amplitude of Field, FLD_AMP

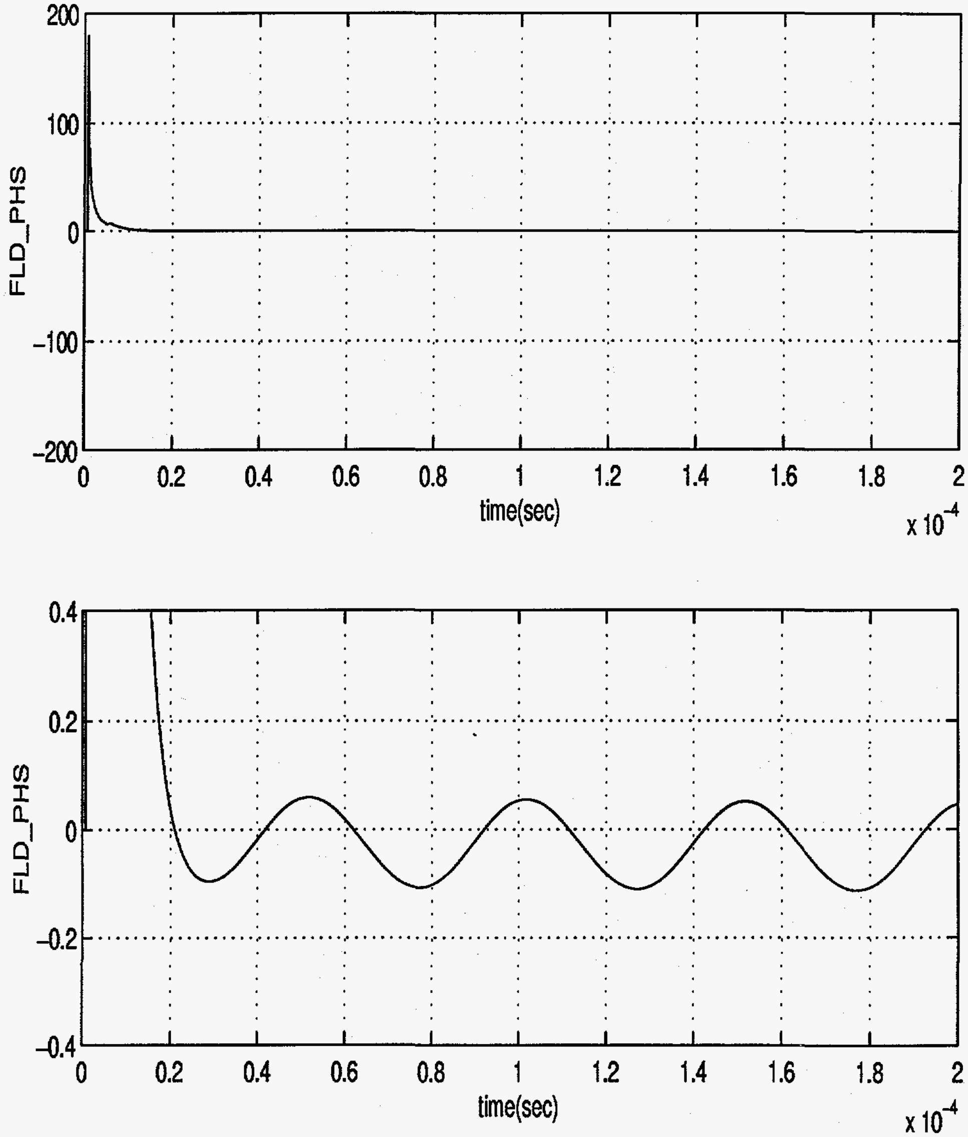

Figure 11: Phase of Field, FLD_PHS

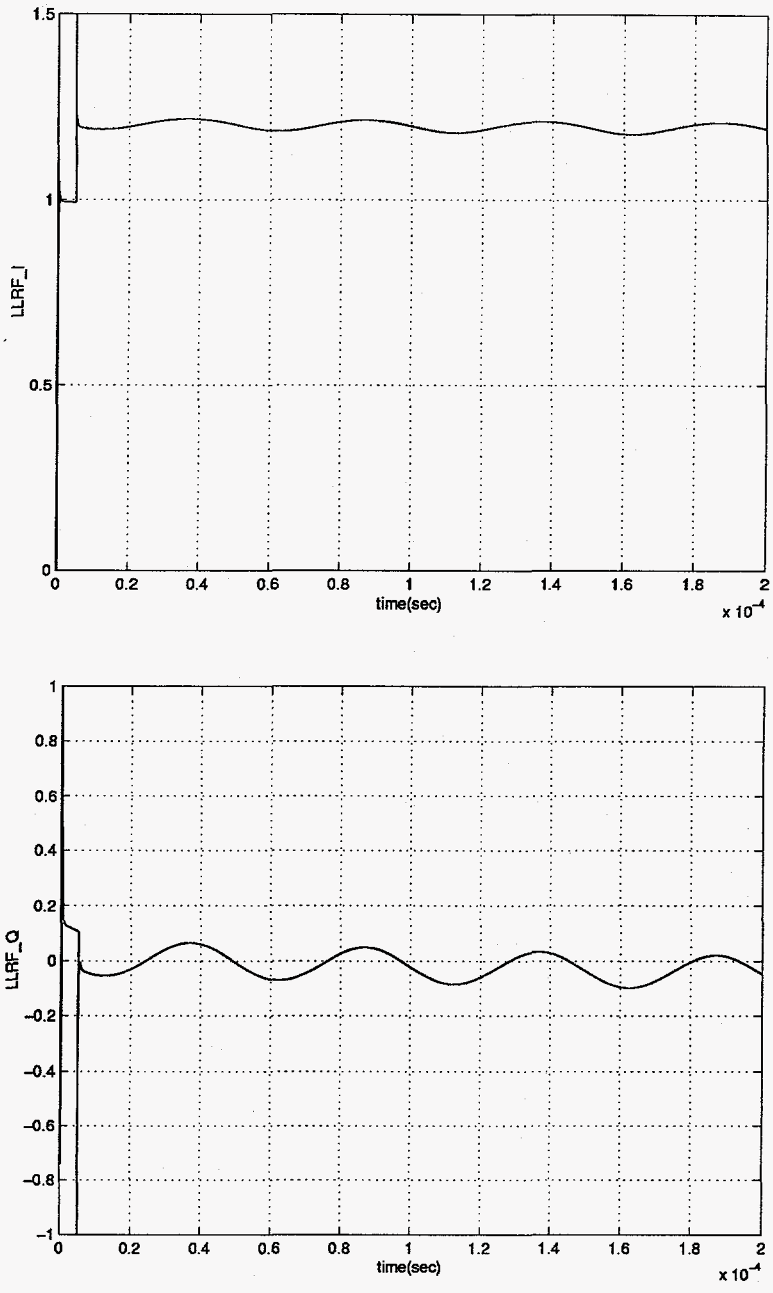

Figure 12: LLRF_I and LLRF_Q

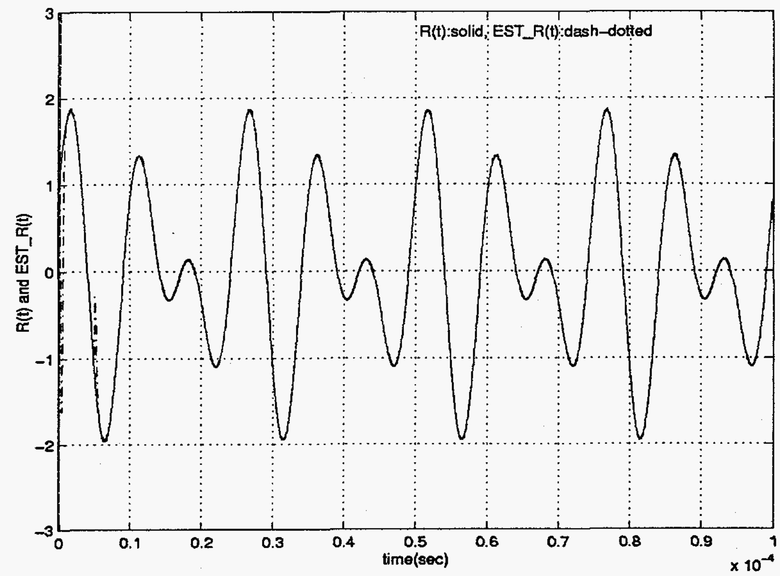

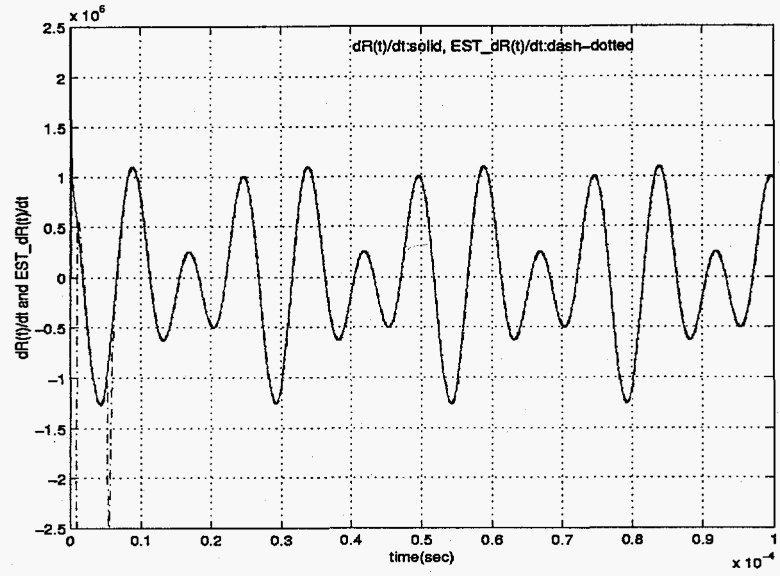

Figure 13: Ripple $R(t)$ and its time derivative $dR(t)/dt$ and their estimates $EST\_R(t)$ and $EST\_dR(t)/dt$

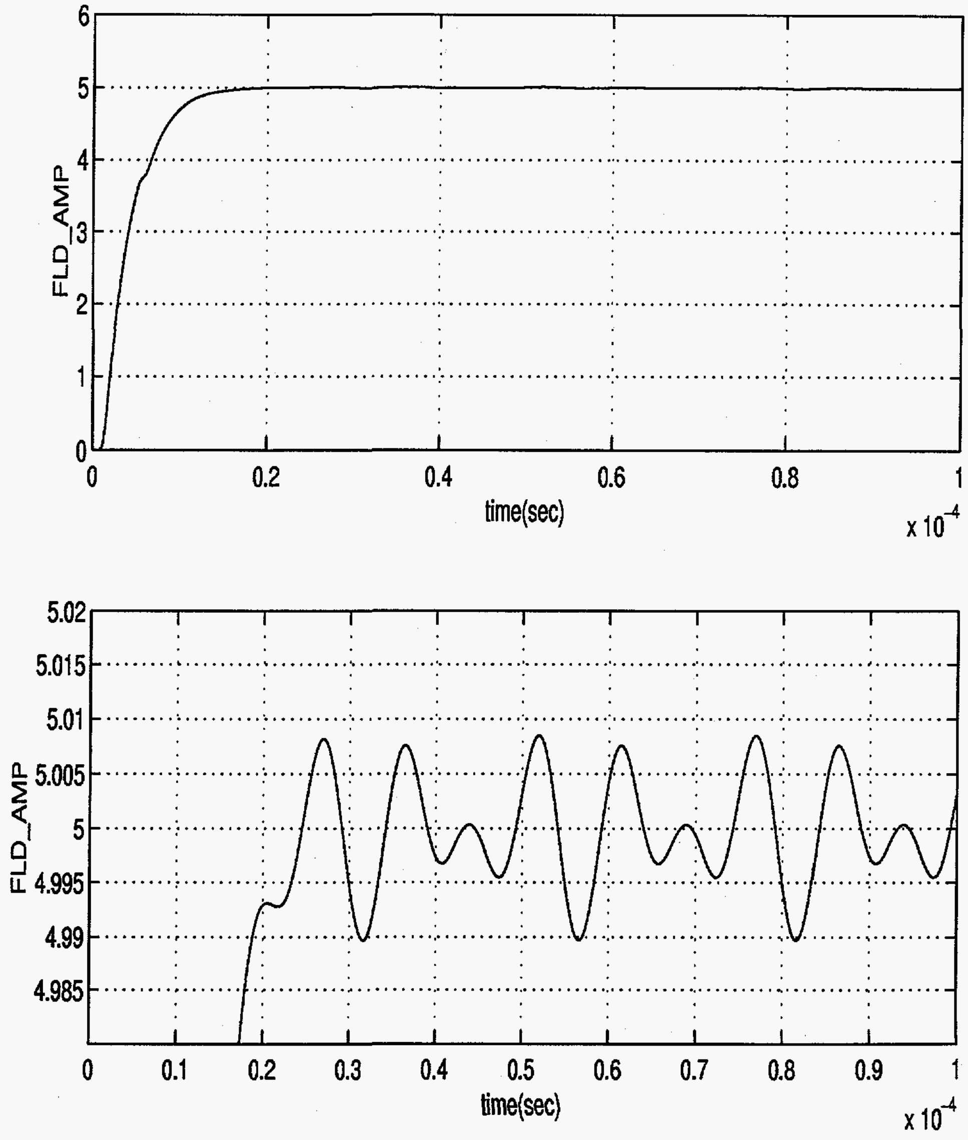

Figure 14: Amplitude of Field, FLD_AMP

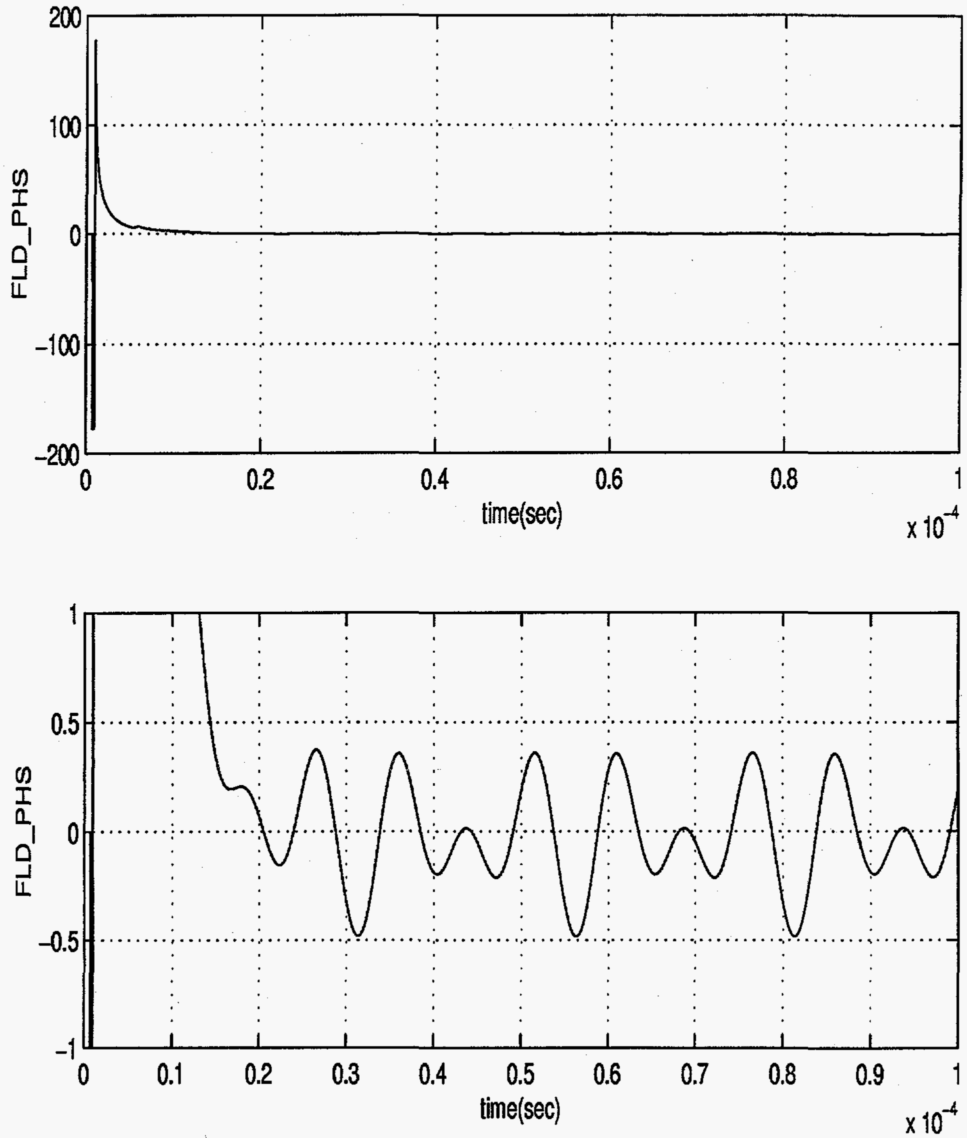

Figure 15: Phase of Field, FLD_PHS

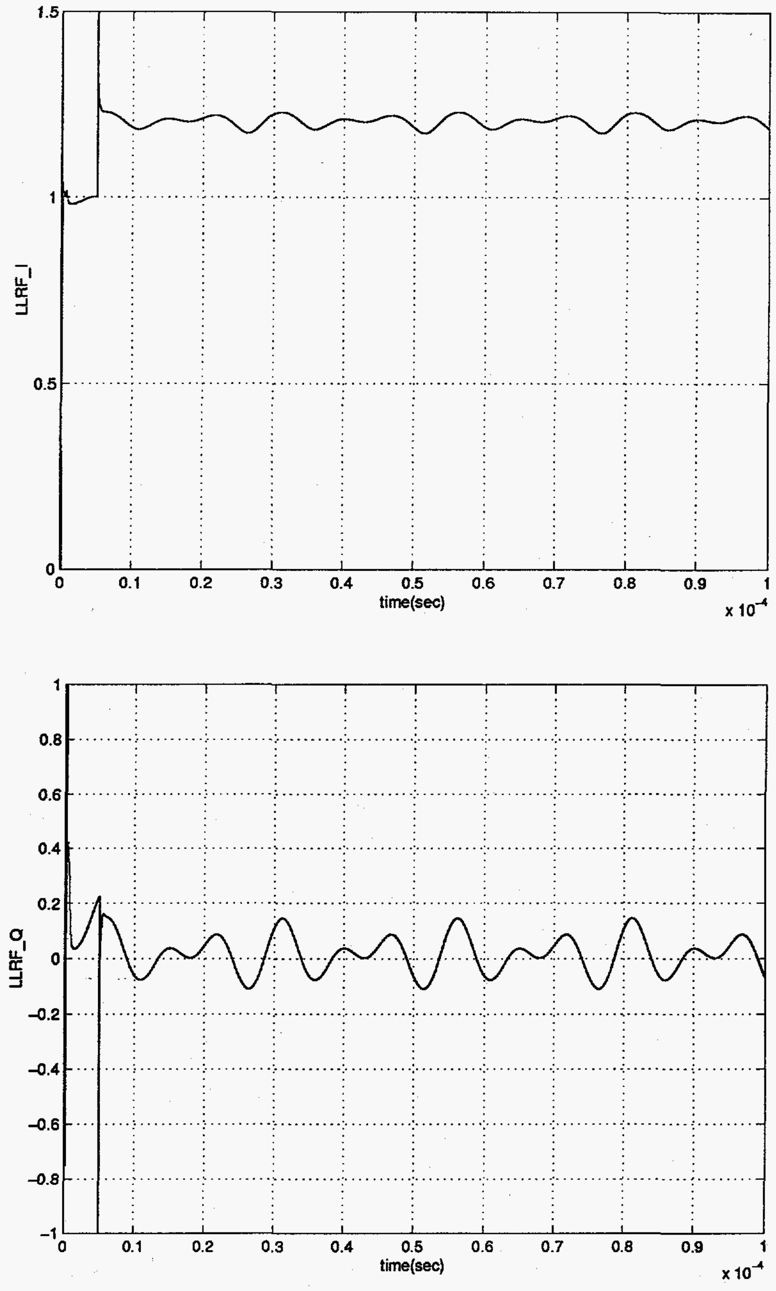

Figure 16: LLRF_I and LLRF_Q